A possible cause of the AO polarity reversal from winter to summer in 2010 and its relation to hemispheric extreme summer weather

By Yuriko Otomi[1], Yoshihiro Tachibana[2,1], and Tetsu Nakamura[3,4]

1: Climate and Ecosystem Dynamics Division, Mie University, Tsu, Japan

2: Japan Agency for Marine-Earth Science and Technology, Yokosuka, Japan

3: Center for Global Environmental Research, National Institute for Environmental Studies, Tsukuba, Japan

4: Now at Faculty of Environmental Earth Science, Hokkaido University, Sapporo, Japan

Accepted in ***Climate Dynamics*** *on 23/04/2012*

Telephone number: +81-463-231-9539

Fax number: +81-463-231-9539

E-mail address: tachi@bio.mie-u.ac.jp

Abstract

In 2010, the Northern Hemisphere, in particular Russia and Japan, experienced an abnormally hot summer characterized by record-breaking warm temperatures and associated with a strongly positive Arctic Oscillation (AO), that is, low pressure in the Arctic and high pressure in the midlatitudes. In contrast, the AO index the previous winter and spring (2009/2010) was record-breaking negative. The AO polarity reversal that began in summer 2010 can explain the abnormally hot summer. The winter sea surface temperatures (SST) in the North Atlantic Ocean showed a tripolar anomaly pattern – warm SST anomalies over the tropics and high latitudes and cold SST anomalies over the midlatitudes – under the influence of the negative AO. The warm SST anomalies continued into summer 2010 because of the large oceanic heat capacity. A model simulation strongly suggested that the AO-related summertime North Atlantic oceanic warm temperature anomalies remotely caused blocking highs to form over Europe, which amplified the positive summertime AO. Thus, a possible cause of the AO polarity reversal might be the "memory" of the negative winter AO in the North Atlantic Ocean, suggesting an interseasonal linkage of the AO in which the oceanic memory of a wintertime negative AO induces a positive AO in the following summer. Understanding of this interseasonal linkage may aid in the long-term prediction of such abnormal summer events.

AO, hot summer 2010, NAM, Atlantic SST, blocking

1. Introduction

In Japan, summer 2010 was the warmest in about 100 years of countrywide measurement records. Moreover, summer 2010 was abnormally hot on a planetary scale. For example, Europe, especially eastern Europe and western Russia, experienced record-breaking hot temperatures, attributed to strong atmospheric blocking over the Euro-Russian region from late June to early August (Matsueda 2011). Additionally, Barriopedro et al. (2011) showed that the spatial extent of the record-breaking temperatures of summer 2010 exceeded the area affected by the previous hottest summer of 2003. Heat anomalies covered almost the entire Eurasian continent in 2010. In contrast, in winter 2009/2010, just a half-year earlier, the continent suffered from anomalously cold weather associated with a record-breaking negative Arctic Oscillation (AO), which is characterized by positive sea level pressure anomalies over the Arctic and negative pressure anomalies over the midlatitudes (Thompson and Wallace 2000). Moreover, in the same winter, a record-breaking negative North Atlantic Oscillation (NAO) caused several severe cold spells over northern and western Europe (Cattiaux et al. 2010). In fact, the strongest negative AO index of the past 30 years was observed in December 2009 (Wang and Chen 2010). This drastic reversal from a record-breaking cold winter to a record-breaking hot summer is preserved in our memory. What if, however, that memory could be preserved not only in our minds but also somewhere on the earth? In particular, might a memory of the strongly negative wintertime 2009/2010 AO have been preserved in the ocean, because of its large thermal heat capacity, which could then be recalled the following summer?

The winter-to-summer evolution of the AO index during 2009/2010 can be summarized as follows: a strongly negative wintertime AO index continued until May, after which it abruptly changed, becoming strongly positive in July and continuing so until the beginning of August. Details of the AO evolution will be described in the following sections. Ogi et al. (2005) pointed out that a strongly positive summertime AO is associated with occurrences of blocking anticyclones, which contributed to the abnormally hot European summer. Trigo et al. (2005) also reported that a blocking anticyclone caused the anomalous hot summer of 2003. The blocking anticyclone over Europe in summer 2003 was shown to be

part of a planetary-scale wave train, extending from Europe to eastern Eurasia (Orsolini and Nikulin 2006). The abrupt change of the AO index from strongly negative to strongly positive in 2010 thus corresponded to the change from the abnormally cold winter of 2009/2010 to the abnormally hot summer of 2010, which shows that the AO index is a good indicator of abnormal weather on a planetary-scale, and that extra-seasonal prediction of the AO is a key to long-term forecasting. In this study, we therefore aimed to examine the cause of the 2010 change in the AO from strongly negative to strongly positive.

2. Data and method

The AO was first defined by Thompson and Wallace (2000) which is based on an invariant EOF spatial pattern throughout the year, and Ogi et al. (2004) identified seasonal variations of the Northern Hemisphere annular mode (SV NAM) from 1958 to 2002 by performing an empirical orthogonal function (EOF) analysis. EOF was applied to a temporal covariance matrix of geopotential height fields for individual calendar months using a zonally averaged monthly geopotential height field from 1000 to 200 hPa for the area poleward of 40°N. The daily time series of the SV NAM index is obtained by projecting daily zonal mean geopotential height anomalies onto the EOF of each month. The time series of the SV NAM index shown in Fig. 1 is calculated by this method.

Ogi et al. (2004) and Tachibana et al. (2010) demonstrated that in winter, but not in summer, the SV NAM accords well with the AO defined by Thompson and Wallace (2000) and used by the Climate Prediction Center of the U.S. National Oceanic and Atmospheric Administration (NOAA/CPC). Ogi et al. (2005) and Tachibana et al. (2010) also demonstrated that the SV NAM successfully captures anomalous summertime weather conditions associated with blocking anticyclones, such as the hot summer in Europe in 2003, whereas the original AO of Thompson and Wallace (2000), mainly reflects atmospheric variabilities in winter and cannot capture such a hot summer. Therefore, Ogi et al. (2005) redefined the summertime SV NAM as the summer AO. In this study, therefore, we adopted the SV NAM index defined by Ogi et al. (2004) as the AO index, and all references to the AO index in this study mean the SV NAM index.

We used daily data of large-scale atmospheric fields from the National Centers for Environmental Prediction/National Center for Atmospheric Research (NCEP/NCAR) reanalysis data set (Kalnay et al. 1996) to calculate the climatology and anomalies of the meteorological field (i.e., temperature, geopotential height, and wind velocity). Monthly means of sea surface temperature (SST) data are from the NOAA_ERSST_V3 data set, provided by NOAA/OAR/ESRL PSD (http://www.esrl.noaa.gov/psd/) (Smith et al. 2008, Xue et al. 2003). We used monthly mean latent and sensible heat flux data of the Japan 25-year Reanalysis (JRA-25) and the JMA Climate Data Assimilation System to examine the atmosphere–ocean interaction (Onogi et al. 2007). Daily and monthly means of outgoing longwave radiation (OLR) are interpolated OLR data provided by NOAA/OAR/ESRL PSD (Liebmann and Smith 1996). Anomaly fields of individual variables are relative to the multi-year mean climatology from 1979 through 2010 for each month.

3. Strongly positive AO days

The winter-to-summer evolution of the AO index (Fig. 1) showed a strongly negative AO in winter 2009/2010 that lasted through May, followed by an abrupt change to strongly positive values in July and August 2010. In particular, the AO index was extremely positive from 10 July to 4 August 2010, coinciding with a period of abnormally hot days in eastern Europe and the Russian far east. Moreover, the AO index in winter and summer accords well with changes in the temperature anomaly for the Eurasian continent over the same period (Fig. 1, lower panel), although the AO index in spring did not accord well with the temperature. Time-mean atmospheric fields during the strongly positive AO period are shown in Fig. 2. The temperature anomaly field at 850 hPa shows two obvious exceptionally hot areas, one centered over eastern Europe and the other over the Russian far east. Between these two hot areas, cold anomaly areas can be seen over central Siberia and the Arctic. At 300 hPa, a negative geopotential height anomaly is seen over the Arctic region that elongates southward toward central Siberia, whereas positive anomalies characterize the midlatitudes of the Northern Hemisphere. Over eastern Europe, Mongolia, the Russian far east, and the eastern North Pacific Ocean the positive anomalies are

particularly strong. This pattern is very similar to the positive summer AO pattern observed during the unusually hot summer of 2003 (Ogi et al. 2005). In summer 2010, the geopotential height contours meandered widely around the Arctic region, indicating that the polar jet stream meandered similarly. In addition, the jet stream split into north and south branches over eastern Europe and the Russian far east, suggesting the existence of a blocking high. At 300 hPa, wave-activity fluxes (Fig. 2a, green arrows) over the polar jet were oriented from Europe to south of Alaska along the longitudinal circle, and they were particularly strong over eastern Europe and the Russian far east, suggesting Rossby wave sources in those areas. The existence of a double jet stream structure is also apparent in the two zonal wind maxima seen at about 72°N and 45°N along 135°E (Fig. 2c). From the surface to the upper troposphere at about 55°N, where the largest negative wind anomaly is observed, the wind direction is easterly. This large-scale pattern in 2010 is consistent with the findings of Ogi at al. (2004), who reported an enhanced double jet in the positive phase of the summer AO.

4. Oceanic footprint left by the previous winter's negative AO

In the North Atlantic Ocean, a tripolar SST anomaly pattern, warm in the high latitudes, cool in the midlatitudes, and warm in the tropics, persisted from January through August 2010 (Fig. 3). This tripolar pattern is typical of a negative wintertime NAO (e.g., Rodwell et al. 1999, Tanimoto and Xie 2002). In fact, the geopotential height anomaly field at 500 hPa in winter (DJF) 2009/2010 showed the typical pattern for the negative phase of the NAO (Fig. 4). The strong negative phase of the AO index in the winter of 2009/2010 corresponded to the negative phase of the NAO (Figs. 4a and 4b). The temperature anomaly at 850 hPa of winter in the region of high-latitude and mid-latitude North Atlantic corresponded well to the total latent and sensible heat flux anomaly in January and February (Figs. 3 and 4c). Similar to the tripolar SST anomaly pattern, the total latent and sensible heat flux anomaly in January and February was also tripolar (Fig. 3): a downward flux anomaly occurred over high latitudes and the tropical North Atlantic, and an upward flux anomaly was observed over the midlatitudes. The downward anomaly in the high latitudes and tropical North Atlantic lasted until

April, but the sign of the latent and sensible heat flux anomaly reversed from downward to upward over the tropical North Atlantic in May and June and over the North Atlantic high latitudes in July and August, whereas the warm SST anomaly in the high latitudes and tropical North Atlantic continued into the summer. The monthly mean tropical North Atlantic SST from January to August was the warmest observed in the 32 years from 1979 to 2010. On the strongly positive AO days, the OLR anomaly over the North Atlantic was strongly negative over the Caribbean Sea (Fig. 5). The negative OLR anomaly area, which was characterized by strong convective activity, roughly coincided with the area of the warm SST and upward sensible and latent heat flux anomalies in summer. In addition, the wind field anomaly in the lower troposphere was cyclonic in the central area of the negative OLR anomaly in the tropical North Atlantic.

5. Steady responses to the oceanic forcing in the Atlantic region

The results presented in sections 3 and 4 suggest that the SST anomaly pattern in the Atlantic Ocean in summer 2010 remotely influenced the midlatitude atmospheric circulation. Many studies have investigated North Atlantic influences on the midlatitudes. For example, Cassou et al. (2005) showed that atmospheric convection over the tropical Atlantic leads to an anticyclonic anomaly over Europe. To make a robust assessment of the SST influence, a sensitivity experiment conducted with a numerical model that simulated the atmospheric responses to a given anomalous SST in the Atlantic region would be useful. However, it is generally difficult to simulate the evolution of a blocking high with an atmospheric general circulation model because of the strong non-linearity of blocking highs. Here we adopted instead a simple linear model, formulated by Watanabe and Kimoto (2000), to simulate the atmospheric response to the ocean. In this model, a spectral primitive equation is linearized about the climatological mean state. We used a version with T42L20 resolution. A steady response X with the basic state $\overline{X}$ is derived by using an equation with the matrix form

$$L(\overline{X})X = Q,$$

where Q is the temperature forcing vector and L is the linear dynamical operator (for details, see appendix A and Watanabe and Kimoto 2000). We defined $\overline{X}$ as the climatological mean in July, derived from the monthly mean NCEP/NCAR reanalysis data set, and Q as the diabatic heating anomalies in July 2010, obtained by a conventional Q1 analysis (Yanai et al. 1973, see appendix B for details) using the 6-h NCEP/NCAR reanalysis data. A model simulation is useful to examine whether the oceanic memory in the Atlantic region is essential to the generation of the blocking high. Thus, we separately calculated Q at levels from 0.7 to 0.3 σ (σ-coordinate system) for the Atlantic Ocean region from 90°W to 30°E (Fig. 6a) and the Eurasian and African continental region from 0°E to 150°E (Fig. 6b) in the Northern Hemisphere. The horizontal distribution of the diabatic heating anomalies in July 2010 (Fig. 6a) is acceptably similar to the SST tripolar pattern (Fig. 3, JA, bottom left). In particular, warmer SST regions (around the British Isles and near the equator) correspond to positive anomalies in the temperature forcings. The coincidence of the regions of warmer SST and positive heating anomalies indicates that the Atlantic Ocean heats the atmosphere in those regions. On the other hand, in the continental region, although heating anomalies are significant over low-latitude Africa where OLR anomalies were negative (Fig. 5), cooling anomalies are dominant in western Russia and northern Europe but with except of Scandinavia.

Figure 7 shows the steady responses of zonal wind and geopotential height at 300 hPa to the given Q. In the responses to the forcing of the Atlantic Ocean, an anticyclonic height anomaly with a maximum amplitude exceeding 30 m is obvious over northern Europe (Fig. 7c), and the corresponding zonal wind anomaly strengthens the climatological double-jet structure (Fig. 7a). On the other hand, in the responses to the forcing of the Eurasian and African continent, a strong cyclonic anomaly is seen over northern Europe/western Russia (Fig. 7d), which may be a counter response to dynamical (i.e., adiabatic) heating due to the blocking high developed there. Thus, our model simulation strongly suggests that atmospheric heating related to the tripolar pattern of the Atlantic SST anomaly is one of the main causes of the blocking high over Europe.

6. Discussion

Taking together the results presented in sections 3, 4, and 5, we suggest that an oceanic memory of the strongly negative wintertime AO may have influenced the strongly positive summertime AO. A negative wintertime NAO would cause warm SST anomalies in high- and low-latitude regions of the Atlantic, as suggested by Xie and Tanimoto (1998) and Tanimoto and Xie (2002). Because the horizontal structures of the NAO and the AO in the Atlantic sector in winter 2009/2010 are similar (See Fig. 4), the strongly negative wintertime AO would maintain the warm SST anomaly in this region. The downward latent and sensible heat flux anomaly over the high latitudes and the tropical Atlantic (Fig. 3) in winter and spring indicates that anomalous heating of the ocean by the atmosphere occurred from winter to spring during the strongly negative phase of the AO in winter 2009/2010. Because the thermal heat capacity of the ocean is large, the sea surface stored this warmth (i.e., the SST anomaly remained positive) into the following summer.

In May and June, the heat flux anomaly changed from downward to upward in the tropics (see Fig. 3), and in July and August, the center of the upward anomaly moved westward. The area of the upward heat flux anomaly coincided with the area of the warm SST anomaly from May to August. The warm SST during the summer following the strongly negative wintertime AO therefore heated the atmosphere, activating atmospheric convection. The OLR anomalies also indicate high convective activity in the tropical Atlantic region (Fig. 5), suggesting a remote influence of the Atlantic SST upon the occurrence of an anticyclone over Europe. This Atlantic SST influence has been pointed out by many studies (e.g., Cassou et al. 2005, García-Serrano et al. 2008). García-Serrano et al. (2008) showed that a midlatitude anticyclonic anomaly related to tropical convection can excite a Rossby wave. Our numerical experiment using the linear model showed that the atmospheric response to the tripolar SST pattern clearly resulted in an anomalous height and wind pattern that caused a blocking high over Europe (Figs. 6 and 7), however, the modeled geopotential amplitude is weaker than the observations. This discrepancy is because a linear model cannot represent the dynamical instability due to, for example, wave–wave interaction. Therefore, the model indicates that although the oceanic memory in the Atlantic is a trigger, by itself it is insufficient to cause a blocking high to develop. Weak,

positive OLR anomalies along the Gulf Stream were associated with anticyclonic surface winds on strongly positive AO days (Fig. 5). The observed wave activity flux (Fig. 2a) also seems to emanate from that region. This midlatitude signature implies that strengthening of the positive geopotential anomalies over Europe was associated with the Atlantic tripolar SST anomaly.

The positive geopotential anomaly in the area of the polar jet stream caused eastward propagation of Rossby waves, and the unusual amplification of Rossby waves might have led to the formation of blocking anticyclones. These findings are in agreement with previous studies. For example, Tachibana et al. (2010) reported that a blocking anticyclone over the Atlantic sector that induces blocking over the Russian Far East is associated with a long-lasting, strongly positive AO caused by wave–mean flow interactions. As a result of these interactions, the positive AO pressure pattern can continue for a long time. In addition, Orsolini and Nikulin (2006) pointed out that the blocking anticyclone over Europe in summer 2003 was part of a wave train extending from Europe to eastern Eurasia. The linear model did not simulate an anticyclonic anomaly in the Russian Far East. To simulate the influence of an anomalous wintertime negative AO on an anomalous positive AO in the following summer due to a long-lasting oceanic memory, an atmosphere–ocean coupled high-resolution model simulation is needed. We reserve this experiment for future studies.

Of course, the set of processes introduced here is just one possible explanation for the formation of the strongly positive summer AO in 2010. For example, summertime SST anomalies in the Mediterranean Sea (Feudale and Shukla 2010) might simultaneously induce a strongly positive summer AO. Although the effect of the oceanic memory of a negative AO during the previous winter might be smaller than the effects of simultaneous events, the previous winter's footprint may at least play a role in the reversal of the AO polarity from a strongly negative wintertime AO to a strongly positive summertime AO. If this reversal pattern recurs, it might be possible to predict the summer AO from the wintertime AO. The more negative the winter AO anomaly is, the deeper the footprint left in the ocean would be, suggesting that a winter-to-summer reversal of the AO might occur only in years when the negative wintertime AO anomaly is large. In addition to an oceanic memory effect, other memory effects such as anomalous snow accumulation on the Eurasian continent or elsewhere in the

Northern Hemisphere, as suggested by Ogi et al. (2003) and Barriopedro et al. (2006), may also contribute to the reversal of AO polarity. To test these possibilities, statistical analyses of multi-year data and simulation by a full coupled atmosphere–ocean–land global climate model are the next step.

Appendix A

A brief description of the linear baroclinic model

In this study, we used a linear baroclinic model (LBM) identical to one used by Watanabe and Kimoto (2000). They exactly linearized primitive equations in which the prognostic variables are vorticity (ζ), divergence (D), temperature (T), and surface pressure ($\pi = \ln P_s$). Using a state vector $X(\zeta, D, T, \pi)$, a dynamical system can be represented as

$$d_t X + (L + NL)X = F, \tag{1}$$

where L and NL are the linear and nonlinear parts of a dynamical operator that consists of, for example, advection, Coriolis, pressure gradient, and dissipation terms. F is a forcing (in this study, we used diabatic heating Q). Now, a state vector X can be decomposed into a basic state $\overline{X}$ and a perturbation part X', i.e., $X = \overline{X} + X'$. Equation (1) is linearized about a basic state $\overline{X}$. Then we consider the steady problem, neglecting the nonlinear part, obtaining a set of linear equations for the perturbation of the prognostic variables X':

$$LX' = F'. \tag{2}$$

Note that a linear dynamical operator L is now a function of the basic state, i.e., $L \equiv L(\overline{X})$, obtained following Hoskins and Karoly (1981). Equation (2) can be solved by using an inverse matrix of L:

$$X' = L^{-1}F'. \tag{3}$$

Equation (3) gives us a steady response to a given forcing. Linearized equations are not necessarily required to obtain a steady response. For a process such as the development of a blocking high, in which internal instability is important, linear responses may be weaker than expected. However, LBM is useful for diagnosing the primary response of the atmosphere without secondary feedback due to, for example, changes in heat fluxes from surfaces.

Appendix B

Estimation of diabatic heating in the atmosphere

Atmospheric diabatic heating can be estimated as a residual term from a heat budget analysis of the thermodynamical equation. Here, diabatic heating Q is defined as follows:

$$Q \equiv C_p (p/p_0)^{\frac{R}{C_p}} \left(\frac{\partial \theta}{\partial t} + v \cdot \nabla \theta + \omega \frac{\partial \theta}{\partial p} \right),$$

where C_p is specific heat of dry air at constant pressure, R gas constant for dry air, p pressure, p_0 standard sea level pressure (= 1000 hPa), θ potential temperature, v horizontal wind vector, and ω pressure velocity. Q includes not only sensible heat but also latent and radiative heat. In general, in the free troposphere, the latent heat associated with the condensation and the evaporation of water vapor is dominant, although the radiative heating may be large in a specific situation such as at the cloud-top.

This estimation method was first introduced by Yanai et al. (1973). They used Q (named Q1 in their study) as an apparent heat source and further defined Q2, which is a residual term of the water vapor budget equation, as an apparent moisture (i.e., latent heat) sink to estimate properties of the tropical cloud cluster from the observed large-scale heat and moisture budget. They also pointed out that this method is useful for determining how a large-scale air is heated diabatically, including both latent and radiative heating.

Acknowledgments

We extend special thanks to M. Honda, H. E. Hori, and J. Inoue for their very helpful comments on this study. We also thank two anonymous reviewers for their valuable comments and suggestions to improve the quality of the paper. This study was supported by Grant-in-Aid for challenging Exploratory Research 22654055, and a part of this study was supported by "Green Network of Excellence" Program (GRENE Program) Arctic Climate Change Research Project.

References

Barriopedro D, García-Herrera R, Hernández E (2006) The role of snow cover in the Northern Hemisphere winter to summer transition. Geophys Res Lett 33:L14708. doi: 10.1029/2006GL025763.

Barriopedro D, Fischer EM, Luterbacher J, Trigo RM, García-Herrera R (2011) The hot summer of 2010: redrawing the temperature record map of Europe. Science 332:220-224. doi: 10.1126/science.1201224.

Cassou C, Terray L, Phillips AS (2005) Tropical Atlantic influence on European heat waves. J Clim 18:2805-2811.

Cattiaux J, Vautard R, Cassou C, Yiou P, Masson-Delmotte V, Codron F (2010) Winter 2010 in Europe: A cold extreme in a warming climate. Geophys Res Lett 37:L20704. doi: 10.1029/2010GL044613.

Feudale L, Shukla J (2010) Influence of sea surface temperature on the European heat wave of 2003 summer. Part I: an observational study. Climate Dynamics 36:1691-1703. DOI: 10.1007/s00382-010-0788-0.

García-Serrano J, Losada T, Rodríguez-Fonseca B, Polo I (2008) Tropical Atlantic variability modes (1979-2002). Part II: Time-evolving atmospheric circulation related to SST-forced tropical convection. J Clim 24:6476-6497.

Hoskins B J, Karoly D J (1981) The steady linear response of a spherical atmosphere to thermal and orographical forcing. J Atmos Sci 38:1179-1196.

Kalnay E et al. (1996) The NCEP/NCAR 40-year reanalysis project. Bull Am Meteorol Soc 77:437-471.

Liebmann B, Smith CA (1996) Description of a complete (interpolated) outgoing longwave radiation dataset. Bull Am Meteorol Soc 77:1275-1277.

Matsueda M (2011) Predictability of Euro-Russian blocking in summer of 2010. Geophys Res Lett 38:L06801. doi: 10.1029/2010GL046557.

Ogi M, Yamazaki K, Tachibana Y (2003) Solar cycle modulation of the seasonal linkage of the North Atlantic Oscillation (NAO). Geophys Res Lett 30:2170. doi: 10.1029/2003GL018545.

Ogi M, Yamazaki K, Tachibana Y (2004) The summertime annular mode in the Northern Hemisphere and its linkage to the winter mode. J Geophys Res 109:D20114. doi: 10.1029/2004JD004514.

Ogi M, Yamazaki K, Tachibana Y (2005) The summer northern annular mode and abnormal summer weather in 2003. Geophys Res Lett 32:L04706. doi: 10.1029/2004GL021528.

Onogi K et al (2007) The JRA-25 reanalysis. J Meteorol Soc Japan 85:369-432.

Orsolini YJ, Nikulin, G (2006) A low-ozone episode during the European heatwave of August 2003. Quart J Roy Meteor Soc 615:667-680. doi: 10.1256/qj.05.30.

Rodwell MJ, Rowell DP, Folland CK (1999) Oceanic forcing of the wintertime North Atlantic Oscillation and European climate. Nature 398:320-323.

Smith TM, Reynolds RW, Peterson TC, Lawrimore J (2008) Improvements to NOAA's historical merged land-ocean surface temperature analysis (1880–2006). J Clim 21:2283-2296.

Tachibana Y, Nakamura T, Komiya H, Takahashi M (2010) Abrupt evolution of the summer Northern Hemisphere annular mode and its association with blocking. J Geophys Res 115:D12125. doi: 10.1029/2009JD012894.

Takaya K, Nakamura H (2001) A formulation of a phase-independent wave-activity flux for stationary and migratory quasigeostrophic eddies on a zonally varying basic flow. J Atmos Sci 58:608-627.

Tanimoto Y, Xie SP (2002) Inter-hemispheric decadal variations in SST, surface wind, heat flux and cloud cover over the Atlantic Ocean. J Meteor Soc Japan 80:1199-1219.

Thompson DWJ, Wallace JM (2000) Annular modes in the extratropical circulation. Part I: Month-to-month variability. J Clim 13:1000-1016.

Trigo RM, García-Herrera R, Díaz J, Trigo IF, Valente MA (2005) How exceptional was the early August 2003 heatwave in France? Geophys Res Lett 32:L10701. doi: 10.1029/2005GL022410.

Wang L, Chen W (2010) Downward Arctic Oscillation signal associated with moderate weak stratospheric polar vortex and the cold December 2009. Geophys Res Lett 37:L09707. doi: 10.1029/2010GL042659.

Watanabe M, Kimoto M (2000) Atmosphere-ocean thermal coupling in the Northern Atlantic: A positive feedback. Q J R Meteorol Soc 126:3343-3369.

Xie SP, Tanimoto Y (1998) A Pan-Atlantic decadal climate oscillation. Geophys Res Lett 25:2185-2188.

Xue Y, Smith TM, Reynolds RW (2003) Interdecadal changes of 30-yr SST normals during 1871-2000. J Clim 16:1601-1612.

Yanai M, Esbensen S, Chu JH (1973) Determination of bulk properties of tropical cloud clusters from large-scale heat and moisture budgets. J Atmos Sci 30:611-627.

Figure Captions

Fig. 1 (top) Time series of the AO index (blue) as defined by Ogi et al. (2004), who called it the SV NAM index. For reference, the conventional AO index reported by NOAA/CPC is shown by the gray line. The vertical axis is dimensionless because the indices are normalized. Tick marks on the horizontal axis indicate the first day of each month. Updated daily time series from 1958 are available at http://tachichi.iiyudana.net/DATA%20HP/AOindex_index.html. (bottom) Time series of the temperature anomaly (K) at 925 hPa averaged northward of 32.5°N over the Eurasian continent. Anomalies are calculated according to the daily climatology of 32 years.

Fig. 2 (a) Time-mean geopotential height at 300 hPa, (b) temperature at 850 hPa (T850), and (c) vertical cross section of the eastward wind component at 135°E in the Northern Hemisphere during strongly positive AO days from 10 July to 4 August 2010. Contours show time-mean values of geopotential height (a, contour interval 100 m), temperature (b, contour interval 5 K), and wind speed (c, contour interval 5 m s^{-1}), and the color shading shows (a) the geopotential height anomaly, (b) the temperature anomaly, and (c) the zonal wind anomaly from climatological temporal means. The green arrows in (a) show the wave activity flux (m^2 s^{-2}) at 300 hPa as formulated by Takaya and Nakamura (2001), with the scale shown by the arrow in the upper right corner.

Fig. 3 Evolution of (left column) SST and its anomaly, and (right column) the sum of the latent and sensible heat fluxes and its anomaly, from January to August 2010. Contours show two-month mean values, and the color shading shows the anomalies (deviations from the climatological

447 temporal mean). JF, January and February; MA, March and April; MJ, May and June; JA, July and
448 August. The contour interval for SST is 3 °C, and that for the flux is 40 Wm^{-2}. Here, a positive
449 flux (i.e., upward flux) is defined as from the ocean to the atmosphere. Red or blue shading in the
450 right panels thus indicates anomalous heating or cooling of the ocean, respectively.

451

452 **Fig. 4** Winter 2009/2010 (December, January, and February) mean geopotential height at 1000
453 hPa (a) and 500 hPa (b) and temperature at 850 hPa (c). Contours show winter mean values of
454 geopotential height (contour interval 50 m) and temperature (contour interval 5 K). The color
455 shading shows the geopotential height anomaly or the temperature anomaly from climatological
456 temporal means.

457

458

459 **Fig. 5** OLR anomaly (color scale, Wm^{-2}), defined as the deviation from the climatological
460 temporal mean, on strongly positive AO days. Arrows show the surface wind anomaly (m s^{-1}) on
461 strongly positive AO days, with the scale shown by the arrow below the lower right corner.

462

463 **Fig. 6** Vertically averaged (from 0.7 to 0.3 σ) diabatic heating derived from a conventional Q1
464 analysis (Yanai et al. 1973). The color scale indicates the heating anomaly (K day^{-1}) in July 2010
465 (deviation from the July climatological mean). (a) Heating anomalies over only the Atlantic Ocean
466 (from 90°W to 30°E, from 0°N to 90°N). (b) Heating anomalies over only the Eurasian and
467 African continent (from 0°E to 150°E, from 0°N to 90°N).

468

469 **Fig. 7** (a) Steady responses of zonal wind at 300 hPa (U300) to the heating anomalies over the
470 Atlantic Ocean, corresponding to those shown in Figure 6a. Red/blue shading indicates
471 positive/negative anomalies with units (m s^{-1}). (b) As in (a) except for responses to the heating
472 anomalies over the Eurasian and African continent, corresponding to those shown in Figure 6b. (c
473 and d) As in (a) and (b) except for geopotential height at 300 hPa (Z300) with units (m).

Figure1

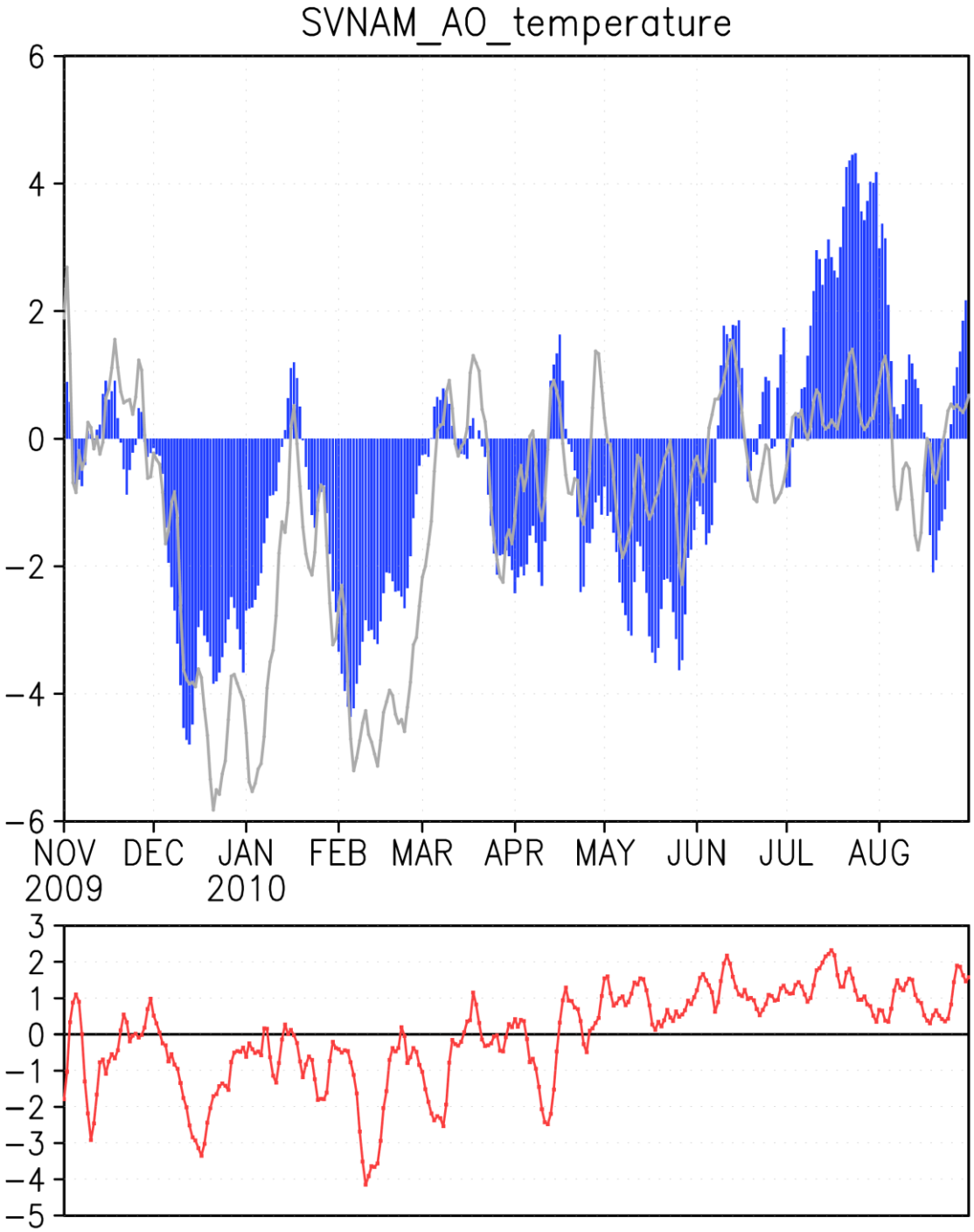

Fig. 1.

Figure2

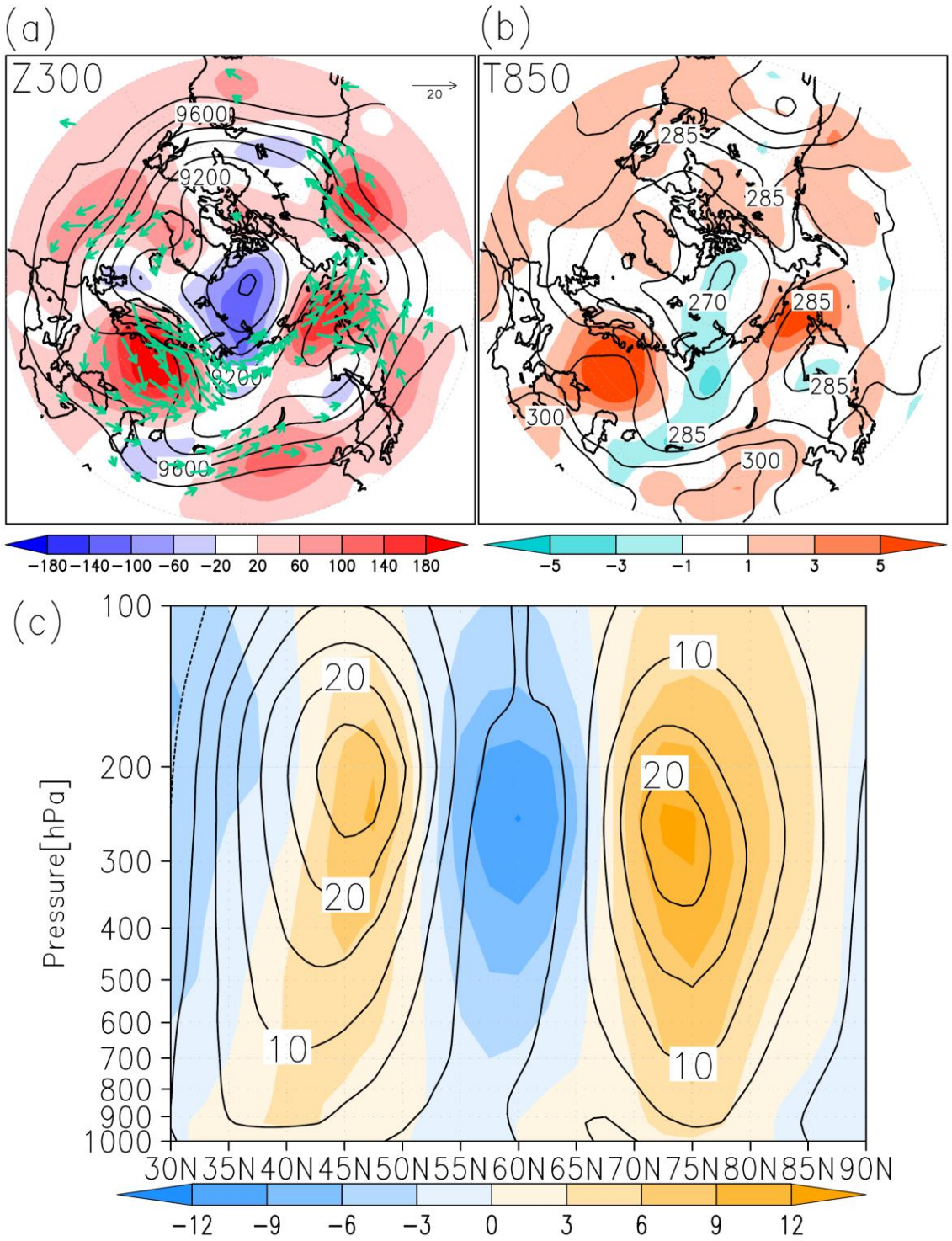

Fig. 2.

Figure3

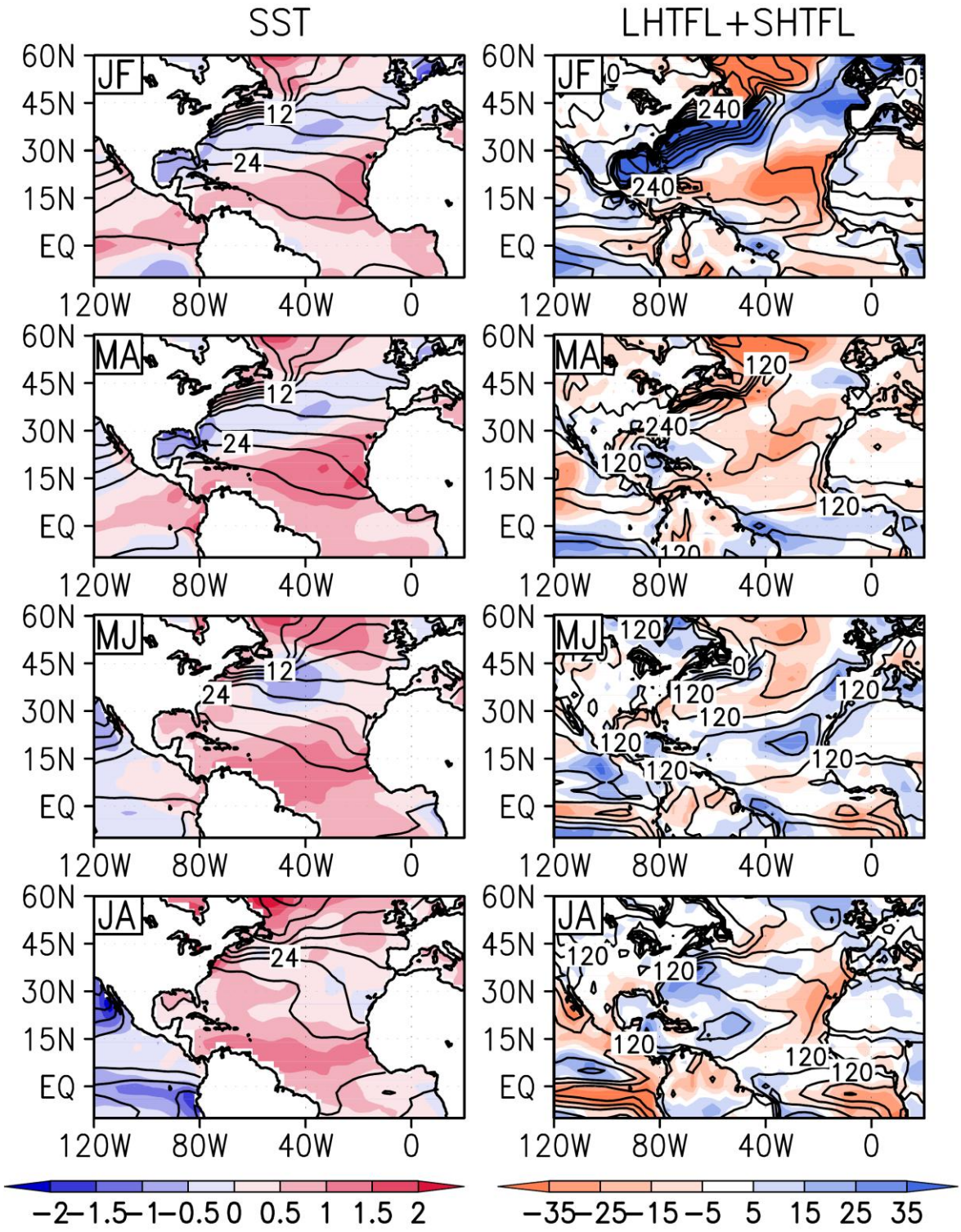

Fig. 3.

Figure4

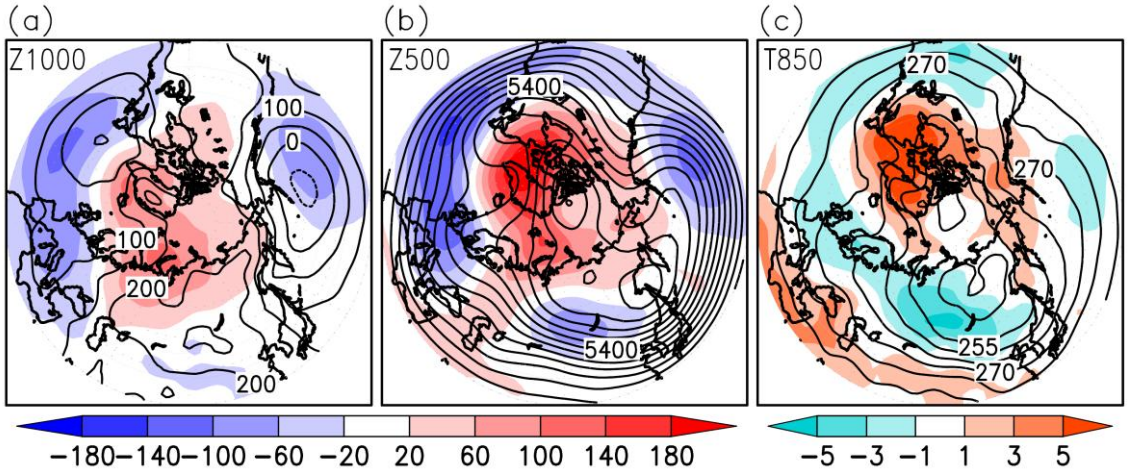

Fig. 4.

Figure5

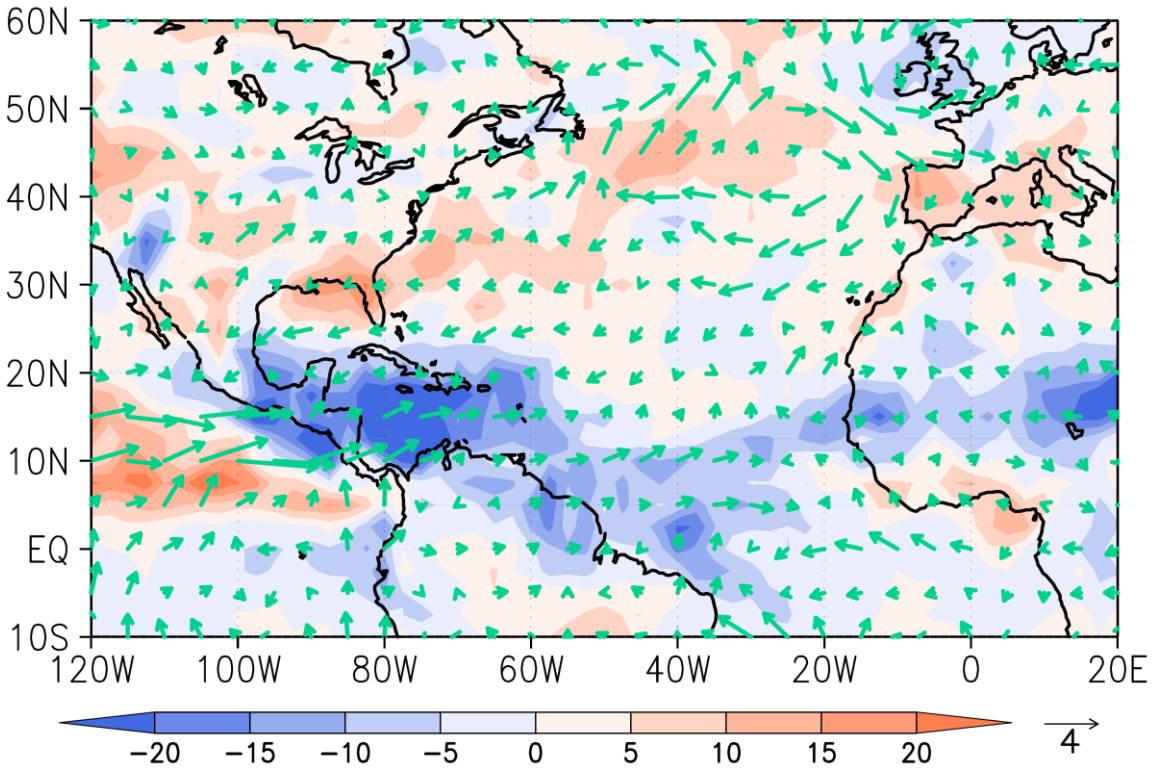

Fig. 5.

Figure6

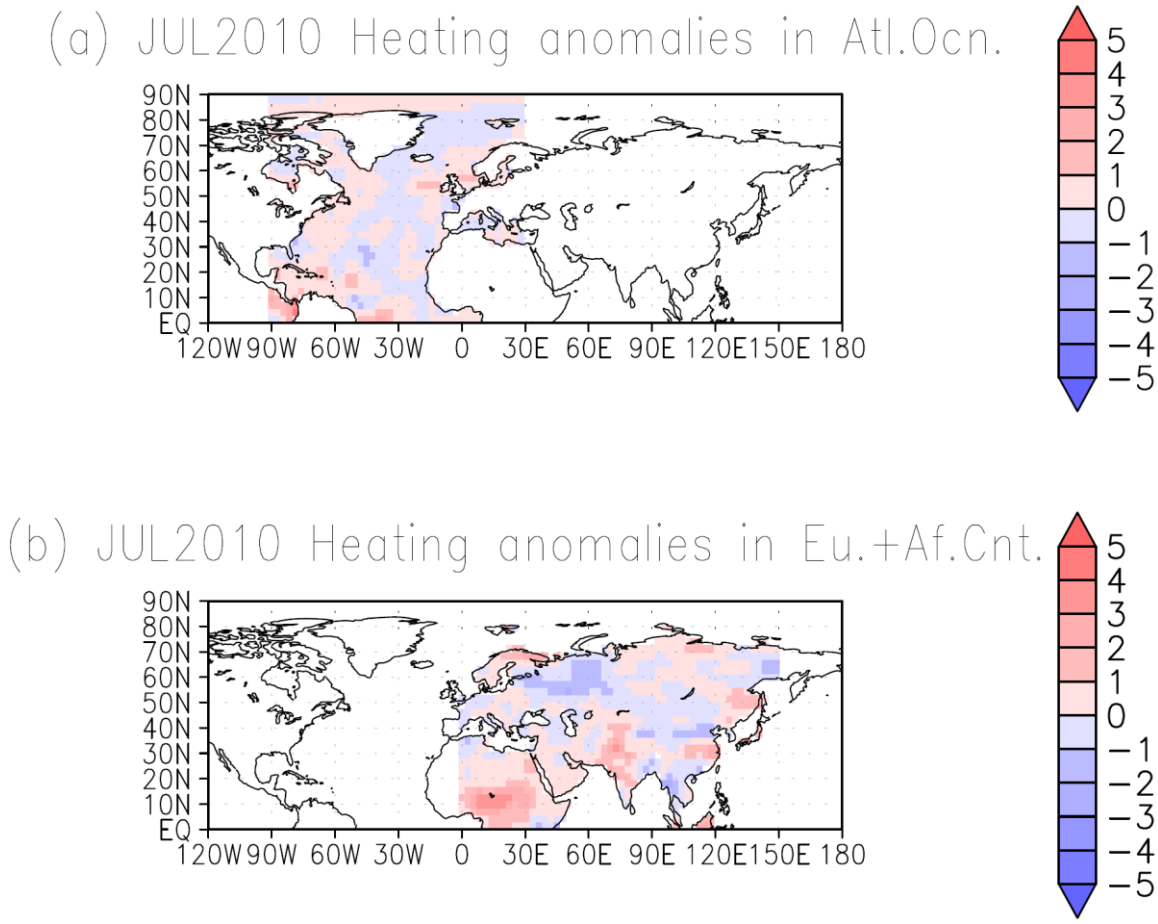

Fig. 6.

Figure7

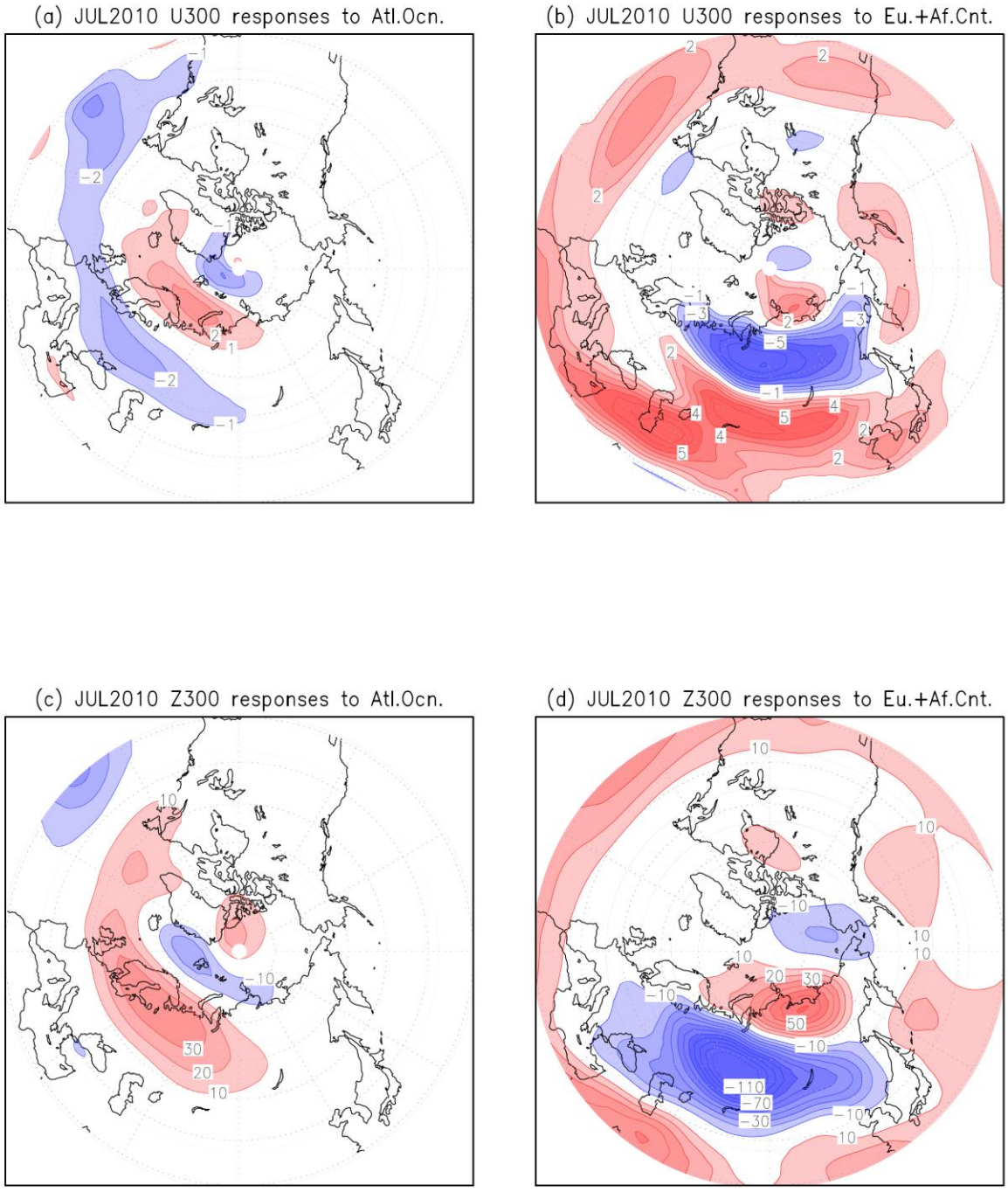

Fig. 7.